15. K. S. Kellogg and P. D. Rowley, *U.S. Geol. Surv. Prof. Pap.* **1498** (1989).
16. J. M. Schopf, *Science* **164**, 63 (1969).
17. D. R. Watts and A. M. Bramall, *Nature* **293**, 638 (1981).
18. A. M. Grunow, D. V. Kent, I. W. D. Dalziel, *J. Geophys. Res.* in press.
19. A. M. Grunow, D. V. Kent, I. W. D. Dalziel, *Earth Planet. Sci. Lett.* **86**, 16 (1987); S. K. Longshaw and D. H. Griffith, *J. Geol. Soc. London* **140**, 945 (1983).
20. E. Stump and P. G. Fitzgerald, *Geology*, in press.
21. B. C. McKelvey, P. N. Webb, D. M. Harwood, M. C. G. Mabin, in *Geological Evolution of Antarctica*, M. R. A. Thomson, J. A. Crame, J. W. Thomson, Eds. (Cambridge Univ. Press, Cambridge, 1991), pp. 675–682; J. C. Behrendt and A. K. Cooper, *Geology* **19**, 315 (1991).
22. A. J. Hurford and P. F. Green, *Isotope Geosci.* **1**, 258 (1983); P. F. Green, 1981, *Nucl. Tracks* **5**, 77 (1981).
23. T. Stump and R. Hall assisted in collection of samples. G. Webers and C. Craddock provided samples of Crashsite quartzite before the field season for determining potential apatite concentrations. Samples were irradiated at the Georgia Institute of Technology Reactor. Supported by NSF grant DPP 8816655. We thank P. Barker for discussions on West Antarctic tectonics and A. Grunow for a preprint (*18*). P. Rowley and an anonymous reviewer improved the quality of this report.

3 June 1991; accepted 6 August 1991

A Dominant Negative Form of Transcription Activator mTFE3 Created by Differential Splicing

CHRISTOPHER ROMAN, LAUREN COHN, KATHRYN CALAME*

Transcription factor E3 (mTFE3) is a murine transcription activator that binds to the intronic enhancer of the immunoglobulin heavy chain gene. A naturally occurring splice product of mTFE3 messenger RNA (mRNA) lacked 105 nucleotides that encode an activation domain; both absolute and relative amounts of long and truncated mRNAs varied in different tissues. Cells were cotransfected with complementary DNAs that encoded the two mRNA forms in amounts that corresponded to the amounts of each mRNA found in different cells. Small changes in substoichiometric amounts of the truncated form of mRNA effected trans-dominant negative modulation of mTFE3 activity. These findings identify a function for differential splicing in the regulation of transcription factor activity.

THE TRANSCRIPTIONAL ACTIVATOR TFE3 (*1*) is one of several structurally related proteins that bind to multiple functionally important sites that include the μE3 or C2 site in the immunoglobulin heavy chain (IgH) enhancer (*1–5*), the C2 site in the IgH V_{H1} (variable) promoter (*4, 5*), the KE3 site in the immunoglobulin κ intronic enhancer (*4, 5*), and the upstream-stimulating factor (USF) binding site in the adenovirus major late promoter (*1, 2, 5*). Studies have identified a transcriptional activation domain near the NH_2-terminus of the human TFE3 protein (*1*). We describe differential splicing of mTFE3 RNA that yields a long form and a truncated form that lacks part of the transcriptional activation domain. Small changes in substoichiometric amounts of the truncated isoform effect down-modulation of the transcriptional activity of mTFE3.

We first isolated an mTFE3 cDNA by screening a λ gt11 expression library with a probe that contained the IgH enhancer μE3 binding site; subsequent overlapping cDNA clones were isolated by DNA hybridization (*5*). Sequence analysis of the cDNAs revealed that we had isolated clones that encoded two isoforms of mTFE3 (Fig. 1A), the murine homolog of human TFE3 (*1*). The mTFE3-S (short) mRNA encodes a polypeptide of 291 amino acids, whereas the mTFE3-L (long) mRNA encodes a polypeptide of 326 amino acids, assuming that the first in-frame methionine is the initiating methionine. Comparison of the human sequence and the murine long-form sequence revealed that the two proteins are nearly identical from the initiator methionine to just COOH-terminal to the leucine zipper (LZ).

Both isoforms contain a basic (B) region, a helix-loop-helix (HLH) region, and an LZ, all of which are important for sequence-specific DNA binding or subunit interactions (*2, 5–8*). We confirmed the ability of mTFE3 to bind DNA and to form multimers by an electrophoretic mobility shift assay (EMSA). A truncated form of mTFE3-S (MTFE3-S-STU), missing the COOH-terminal 120 amino acids but retaining the B-HLH-LZ region, and MTFE3-L were synthesized in vitro. We subjected reticulocyte lysate extracts to an EMSA using an IgH enhancer fragment that contained the μE3 site as a probe. Lysates programmed with either mTFE3-L or mTFE3-S-STU RNA showed DNA-protein complexes that had mobilities consistent with the sizes of the two proteins and that were not present in unprogrammed lysate (Fig. 2, lanes 1, 2, and 4). Lysate programmed with both mTFE3-L and mTFE3-S-STU showed a complex of intermediate mobility (Fig. 2, lane 3). We conclude that both mTFE3-L and mTFE3-S can bind the IgH μE3 site with similar affinity and that mTFE3-L and mTFE3-S can form heteromultimers that also bind the μE3 site with an affinity similar to that of homomultimers.

Fusion of a heterologous DNA-binding domain (GAL4) to regions of TFE3 allowed the identification of a 126–amino acid transcriptional activation domain (*1*). This region contains a stretch of amino acids with a net negative charge that could form an amphipathic helix (underlined in Fig. 1B), which could be a transcriptional acti-

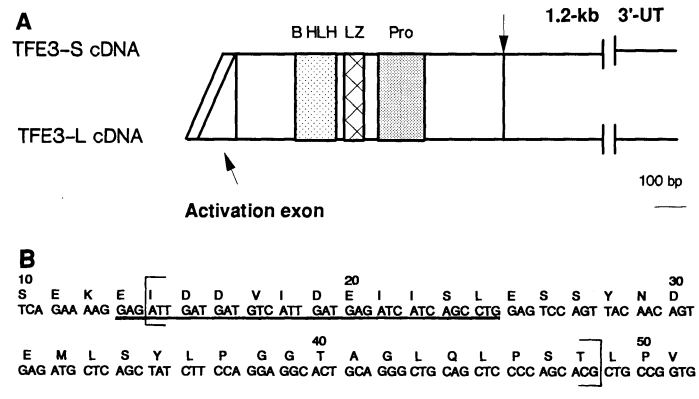

Fig. 1. Structure of mTFE3. (**A**) Schematic representation of mTFE3 cDNAs. Both reading frames terminate at the downward vertical arrow as indicated and contain 1.2 kb of 3′ untranslated sequence (UT). The two cDNAs are identical except for the activation exon. (**B**) Sequence of the NH_2-terminus of mTFE3-L. The numbers above the amino acids mark their positions relative to the initiating methionine. The sequence of the activation exon is bracketed. The underlined sequence represents the putative amphiphatic helix (*1*). Abbreviations for the amino acid residues are as follows: A, Ala; C, Cys; D, Asp; E, Glu; F, Phe; G, Gly; H, His; I, Ile; K, Lys; L, Leu; M, Met; N, Asn; P, Pro; Q, Gln; R, Arg; S, Ser; T, Thr; V, Val; W, Trp; and Y, Tyr.

C. Roman, Department of Biological Chemistry, University of California, Los Angeles, CA 90024.
L. Cohn, Department of Medicine, Columbia University College of Physicians and Surgeons, New York, NY 10032.
K. Calame, Department of Biological Chemistry, University of California, Los Angeles, CA 90024, and Departments of Microbiology, Biochemistry, and Molecular Biophysics, Columbia University College of Physicians and Surgeons, New York, NY 10032.

*To whom correspondence should be addressed.

vation domains (*9*). The polypeptide encoded by mTFE3-S mRNA lacks 35 amino acids (bracketed in Fig. 1B); these include the potential amphipathic helix.

We suspected that the two cDNAs were generated by a naturally occurring splicing event and that the transcriptional activation capability of the polypeptide encoded by mTFE3-S mRNA would be less than that of mTFE3-L. To compare the ability of the two proteins to activate transcription, we performed cotransfection experiments with a chloramphenicol acetyltransferase (CAT) gene controlled by four μE3 sites inserted 5′ to a minimal promoter as a reporter (*1, 10*) (Fig. 3). The mTFE3 cDNAs were expressed from pSV2A (*1, 11*), a simian virus 40 (SV40) expression plasmid that contained mTFE3-S or mTFE3-L cDNA (*12*). The reporter plasmid alone showed low basal activity probably due to endogenous μE3 binding proteins. Cotransfection of the reporter with pSV2A–mTFE3-L showed greater than 11-fold stimulation of CAT activity over the basal amount (Fig. 3). The dependency of this effect on μE3 sites was demonstrated by the lack of activation of a reporter that contained mutant μE3 sites that cannot bind mTFE3 in vitro (*1, 13*). Furthermore, ribonuclease (RNase) protection assays demonstrated that basal and mTFE3-induced CAT transcripts were correctly initiated (*13*). Thus, mTFE3, like the human homolog, is a transcription activator. However, pSV2A–mTFE3-S stimulated transcription only 3.6-fold over the basal amount (Fig. 3). This represents an intrinsic difference in factor activity because the data show that in the range used both pSV2A–mTFE3-L and pSV2A–mTFE3-S functionally saturated the reporter. The activating ability of pSV2A–mTFE3-S is less than one-third of the activating ability of pSV2A-mTFE3-L; this demonstrates that the region missing from mTFE3-S is important for transcriptional activation, confirming results with human mTFE3 (*1*). However, because mTFE3-S retains some ability to trans-activate, we expect that other regions of the protein, possibly a proline-rich region (Pro) COOH-terminal to the LZ, also participate in transcriptional activation.

The mTFE3-L and mTFE3-S cDNAs are identical in regions both 5′ and 3′ of the 105-bp portion missing from mTFE3-S; furthermore, genomic DNA blots with these cDNAs used as probes show hybridization to a single gene (*5*). These data are most consistent with the possibility that the two isoforms are generated by differential splicing of a single transcript. To demonstrate this directly, we isolated genomic clones and determined the exon structure of the gene in the region where mTFE3-L and mTFE3-S differ. Sequence analysis revealed that the 105-bp region present in mTFE3-L cDNA is indeed encoded by a separate exon (Fig. 4).

We wished to confirm that both mTFE3-S and mTFE3-L cDNAs represented mRNAs present in normal tissues and to determine the amounts of these isoforms in various tissues. Therefore, we designed an RNase protection probe to distinguish between the protected fragments generated by hybridization to mTFE3-L mRNA (380 nucleotides) and mTFE3-S mRNA (250 nucleotides) (Fig. 5A). Analysis of total RNA from various sources (Fig. 5B) showed both predicted bands, thus confirming that our two cDNA clones represent endogenous mRNA species. Results from several experiments were quantitated and normalized for the amount of RNA in each lane with a glyceraldehyde phosphate dehydrogenase (GAPDH) probe (Fig. 5, B and C). The mTFE3 mRNA was present in all cells tested, consistent with reports that show that proteins that bind to the μE3 and USF sites have a ubiquitous distribution. The total amount of mTFE3 mRNA varied over 20-fold (Fig. 5C), and the percent contributed by mTFE3-S transcripts varied from almost 20% in liver to 2 to 5% in lymphoid cells (Fig. 5D).

The low percentage of mTFE3-S mRNA raised questions about whether differential splicing of mTFE3 RNA had physiological significance. In other cases, such as with FosB (*14*) and CREB (adenosine 3′,5′-monophosphate response element–binding protein) (*15*), the transcripts that encode forms with lower activity are present in either equimolar amounts or in molar excess. If in these cases protein concentration were proportional to mRNA, an inactive form might displace the active form at the binding site. However, a strong effect would not be expected to result from submolar amounts of mTFE3-S mRNA if inhibition occurred by a simple displacement mechanism. Thus, we determined whether substoichiometric amounts of mTFE3-S mRNA affected the transcriptional activation ability of mTFE3. We performed cotransfection experiments in which expression constructs pSV2A–mTFE3-S and pSV2A–mTFE3-L were mixed at varying ratios, including low ratios of pSV2A–mTFE3-S that corre-

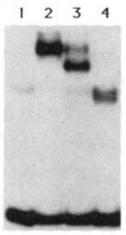

Fig. 2. The mTFE3-L and mTFE3-S proteins form heteromultimers that bind DNA. In vitro–transcribed RNAs encoding full-length mTFE3-L and mTFE3-S-STU, which is truncated COOH-terminal to the LZ region at amino acid 225, were translated in reticulocyte lysates; aliquots of the lysate were incubated with the radiolabeled Pvu II–Dde I IgH enhancer fragment, and DNA-protein complexes were resolved by EMSA (*5*). The DNA-binding specificities of mTFE3-L and mTFE3-S to the μE3 site have been determined by competition and footprinting (*5*). SDS–polyacrylamide gel electrophoresis analysis revealed that all polypeptides were synthesized in equivalent amounts (*13*). Lane 1, naive extract; lane 2, mTFE3-L; lane 3, mTFE3-L plus mTFE3-S-STU; and lane 4, mTFE3-S-STU.

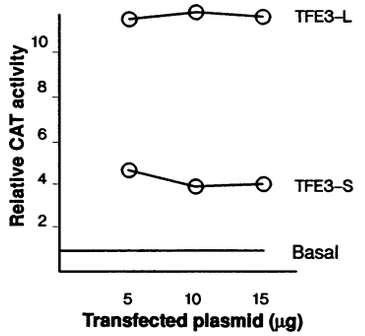

Fig. 3. Different intrinsic transcriptional activating abilities of mTFE3-L and mTFE3-S. The in vivo cDNA expression vectors pSV2A–mTFE3-S and pSV2A–mTFE3-L were constructed as described (*12*) and introduced into NIH 3T3 cells by calcium phosphate–mediated transfection as described (*25, 26*). The indicated amounts of either pSVA–mTFE3-L or pSVA–mTFE3-S were cotransfected with the CAT reporter construct (10 μg). The mutant and wild-type μE3-dependent CAT constructs contained four copies of either wild-type or mutant μE3 site oligonucleotides inserted 5′ of the minimal alkaline phosphatase promoter driving the CAT gene (*1, 10*). Basal activity was set at 1. One representative experiment is shown. The difference between mTFE3-L and mTFE3-S activity remained virtually constant; from 13 pairs of transfectants, the difference in activity (±SD) was 3.5- ± 0.5-fold. No CAT activity was detectable with a mutant μE3 site reporter construct when transfected alone or with the cDNA constructs (*1, 13*).

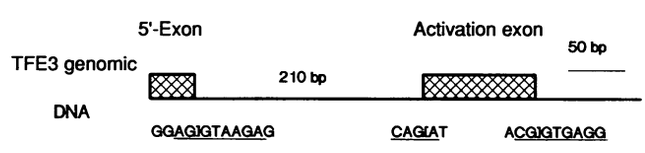

Fig. 4. Schematic representation of the structure of the genomic sequence. Exons are shown as cross-hatched boxes with the sequence of splice-site junctions shown underneath them. The putative splice-site consensus homologies are underlined. Exon boundaries are shown by brackets.

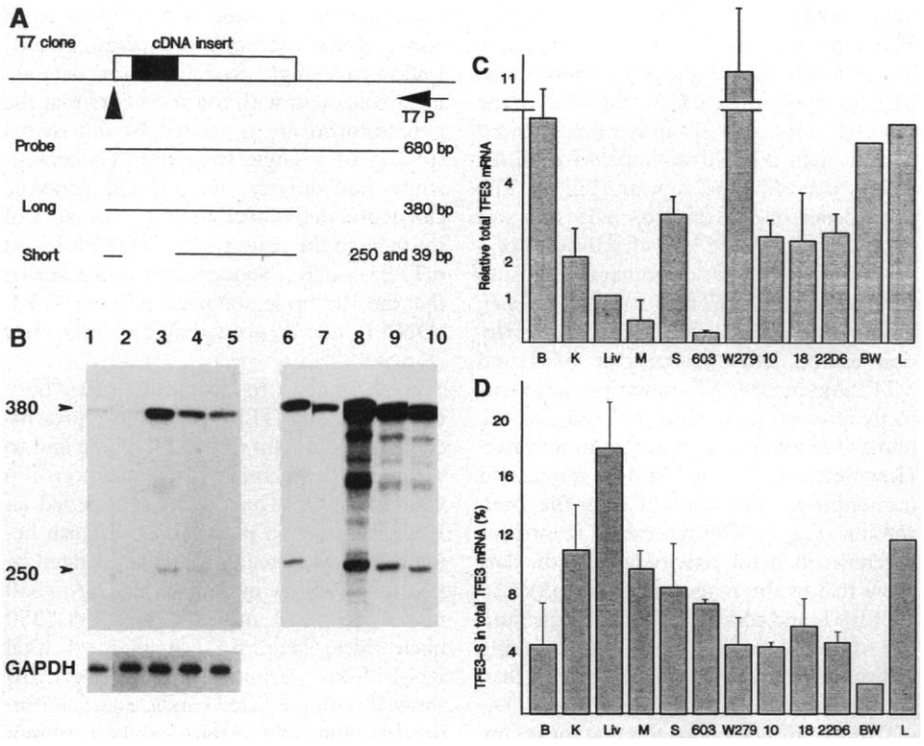

Fig. 5. Riboprobe analysis of mTFE3 transcripts. (**A**) Riboprobe assay. The riboprobe template contained 380 bp of mTFE3-L cDNA linearized at a unique Nco I site (which contains the codon for the initiating methionine) indicated by the vertical arrow. The cDNA coding sequence is represented by a rectangle; the filled region represents the sequences unique to mTFE3-L. The sizes of the predicted bands for mTFE3-L (long) and mTFE3-S (short) are shown. The template also includes heterologous DNA 3′ to the mTFE3 sequence, which was shown not to hybridize to any transcripts (*13*). T7 RNA polymerase–generated antisense riboprobe homogeneously labeled with [α-^{32}P]uridine triphosphate was hybridized with total RNA from the various samples, the samples were digested with RNase A and T1 and the protected fragments were visualized and quantitated as described (*27*). We normalized the amount of mTFE3 RNA species for probe length. (**B**) A typical experiment showing the protected fragments from several tissues. Arrowheads indicate the 380-nucleotide and 250-nucleotide bands indicative of hybridization of the riboprobe to the mTFE3-L and mTFE3-S transcripts, respectively. Lanes 1 and 6, liver; lanes 2 and 7, M603; lanes 3 and 8, WEHI 279; lanes 4 and 9, 300-10 (*28*); and lanes 5 and 10, 300-18 (*28*). Lanes 6 to 10 show a longer exposure time of the same lanes as in 1 to 5. We used the GAPDH probe at the bottom to normalize the results for Fig. 5C. (**C**) Bar graph of the relative amounts of mTFE3 transcripts in the indicated normal murine adult tissues and cell lines as determined by RNase protection analysis (n = 3; error bars indicate SD). (**D**) Levels of mTFE3-S transcript expressed as a percent of the total mTFE3 transcript (mTFE3-S + mTFE3-L) for the indicated samples (n = 3; error bars indicate SD). B, brain; K, kidney; Liv, liver; M, muscle; S, spleen; 603, plasmacytoma M303 passaged as a tumor; W279, B cell line WEHI 279; 10 and 18, pro–B cell lines 300-10 and 300-18, respectively; 22D6, pro–B cell line (*28*); BW, T cell line BW5147; and L, L cells.

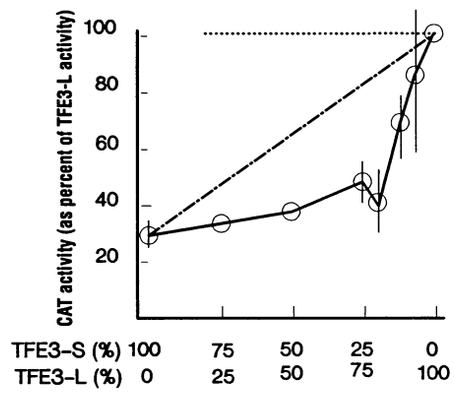

Fig. 6. Transcriptional activation by varying ratios of mTFE3-S and mTFE3-L. The indicated ratios of mTFE3-S and mTFE3-L were cotransfected at saturating concentrations (10 μg) with the wild-type μE3-dependent promoter construct (10 μg). The results compiled from four independent experiments performed with different preparations of expression constructs are shown (solid line). For each set, 100% mTFE3-L was defined as 100% activity, and other points were expressed as a percent relative to this control. With 100% mTFE3-S (S), the percent transcriptional activation (±SD) for four trials was 28% ± 4%; with 25% S, 48% ± 7%; with 20% S, 42% ± 10%; with 12.5% S, 68% ± 10%; and with 6.25% S, 85% ± 23%. We obtained the values of 75% S and 50% S by averaging the values of two exper-iments (for 50% S, 33% and 40%; for 75% S, 40% and 28%). Essentially the same values were obtained in transfections where selected points were repeated five times in the same assay with different preparations of each expression vector. In these transfections, the values were as follows (n = 5; ±SD; $P < 0.05$ relative to 100% mTFE3-L): experiment 1, 100% mTFE3-L (L), 100% ± 16%; 100% mTFE3-S, 25.6% ± 6.2%; 25%, 40% ± 10%; experiment 2: 20% S, 42% ± 10%; 100% L, 100% ± 11%. The dotted line indicates CAT activity observed with L alone; the dashed line indicates CAT activity calculated for varying proportions of L and S, assuming each acted independently and in proportion to the amount of plasmid transfected.

sponded to mRNA ratios found in different tissues (Fig. 5, B through D). Using a polymerase chain reaction (PCR)–based assay, we confirmed that relative concentrations of exogeneous mTFE3-L and mTFE3-S mRNA corresponded to the relative concentrations of DNA transfected (*16*). We performed cotransfections with saturating amounts of mTFE3 vectors to ensure that the measured activity depended on the activity of the mTFE3 mixture and not on different absolute amounts of mTFE3.

The results show that addition of pSV2A–mTFE3-S lowered the ability of a pSV2A–mTFE3-L–mTFE3-S mixture to activate transcription relative to pSV2A–mTFE3-L alone (Fig. 6). Even when substoichiometric amounts (12.5 to 20%) of pSV2A–mTFE3-S were present, activation was less than would be predicted if each form of mTFE3 acted independently and in proportion to the amount of vector transfected. Because the low-activity phenotype (mTFE3-S) is dominant over the high-activity phenotype (mTFE3-L), this indicates trans-dominant negative modulation. The cotransfections duplicate the range of mTFE3-S–mTFE3-L mRNA ratios found by RNase protection in different tissues (Fig. 5D), and the results show that small changes in percent mTFE3-S mRNA in this range have at least a twofold effect. This finding suggests that the trans-dominant negative effect of mTFE3-S may be physiologically important for any gene dependent on mTFE3 and further suggests that it is unnecessary for cells to express more than about 20% mTFE3-S mRNA because larger amounts do not have significantly different effects.

Our results establish the trans-dominant negative effect of mTFE3-S mRNA but do not establish the mechanism responsible for it. It is possible that mTFE3-S has higher affinity for the μE3 site, allowing it to functionally displace mTFE3-L. However, in vitro protein–binding studies show that both polypeptides bind efficiently to the μE3 site (Fig. 2). It is also possible that the two proteins are differentially stable, so that the percent of mTFE3-S protein may be higher than the percent of mTFE3-S mRNA. We have been unable to determine whether exogenous mTFE3 protein concentrations correspond to that of the mRNA.

Another model rests on the premise that transcriptionally active mTFE3 protein exists as a multimer and that the activating ability of mixed multimers is reduced by mTFE3-S subunits. This model would explain how substoichiometric amounts of mTFE3-S may affect the activating ability of mTFE3-L. The mTFE3 protein contains

both the HLH and LZ motifs which are protein-protein interaction domains (*2, 6, 8, 17*). Indeed, we demonstrated (Fig. 2) that mTFE3-L can form heteromultimers with mTFE3-S. Furthermore, the B-HLH protein MyoD and protein products of Achete-Scute are negatively modulated by formation of mixed multimers with HLH proteins Id and Extramacrochaete (*18*). However, the phenomenon we report is different because mTFE3 heteromultimers bind DNA, retain low activation capability, and are generated from the same gene.

Although many transcription factors appear to be controlled at the transcriptional level, regulation at other levels is necessary to avoid an endless progression of transcriptionally controlled events. Several transcriptional regulators encoded by alternatively spliced mRNAs have diverse phenotypes (*14, 15, 19–24*). Among these are the viral gene products E1A (*19*) and E2 (*20*), the homeobox gene product XIHbox-1 (*21*), c-Myb (*22*), Erb-A (*23*), and E2A (*24*). A trans-dominant effect has been noted for an alternative splice product of FosB that decreases full-length FosB activity twofold in cotransfection assays in which ratios of the two forms reflect physiological ratios (*14*). Differential splicing is emerging as an important posttranscriptional control point for the regulation of different aspects of transcription factor activity.

REFERENCES AND NOTES

1. H. Beckmann, L.-K. Su, T. Kadesch, *Genes Dev.* **4**, 167 (1990).
2. P. D. Gregor, M. Sawadago, R. G. Roeder, *ibid.*, p. 1730.
3. C. S. Carr and P. A. Sharp, *Mol. Cell. Biol.* **10**, 4384 (1990).
4. C. Peterson and K. Calame, *ibid.* **9**, 776 (1989).
5. C. Roman, S. Artandi, C. L. Cooper, S. Blain, K. Calame, in preparation.
6. C. Murre, P. Schonleber-McCaw, D. Baltimore, *Cell* **56**, 777 (1989).
7. C. Murre *et al.*, *ibid.* **58**, 537 (1989).
8. A. Voronova and D. Baltimore, *Proc. Natl. Acad. Sci. U.S.A.* **87**, 4722 (1990).
9. E. Giniger and M. Ptashne, *Nature* **330**, 670 (1987); J. Ma and M. Ptashne, *Cell* **48**, 847 (1987).
10. M. Kiledjian and T. Kadesch, *Nucleic Acids Res.* **18**, 957 (1990).
11. J. R. deWet, K. V. Wood, M. DeLuca, D. R. Helsinki, S. Subramani, *Mol. Cell. Biol.* **7**, 725 (1987).
12. The cDNAs described in Fig. 1 were inserted into pBS-ATG (*6*) a vector that supplies a translation initiation site. The initiating methionine in pBS-ATG corresponds to the initiating methionine of the cDNAs. There are no amino acids derived from the pBS-ATG vector in the coding sequences. We constructed the plasmids pSV2A–mTFE3-S and pSV2A–mTFE3-L by insertion of the Hind III–Eco RI fragment from the pBS-ATG–cDNA vectors that contained the entirety of the cDNA (2.1 kb) and inserted them into pSV2A (*1, 11*) that had been linearized with Bam HI and Hind III and end-filled. These vectors drive transcription of the cDNA by the SV40 enhancer and early promoter.
13. C. Roman and K. Calame, unpublished data.
14. Y. Nakabeppu and D. Nathans, *Cell* **64**, 751 (1991); J. Yen and I. M. Verma, *Proc. Natl. Acad. Sci. U.S.A.* **88**, 5077 (1991).
15. K. K. Yamamoto, G. A. Gonzalez, P. Menzel, J. Rivier, M. R. Montminy, *Cell* **60**, 611 (1990).
16. For a mix of 80% mTFE3-L– and 20% mTFE3-S–transfected expression vectors, an exogenous RNA ratio of 78.3% mTFE3-L and 21.6% mTFE3-S (n = 3, ±SD of 6.3%) was obtained.
17. W. H. Landschulz, P. F. Johnson, S. L. McKnight, *Science* **243**, 1681 (1989).
18. N. Jones, *Cell* **61**, 9 (1990); J. Garrell and J. Modelell, *ibid.*, p. 39; H. M. Ellis, D. R. Spann, J. W. Posakony, *ibid.*, p. 27; R. Benezra, R. L. Davis, D. Lockshon, D. L. Turner, H. Weintraub, *ibid.*, p. 49.
19. L. W. Lillie, M. Green, M. R. Green, *ibid.* **46**, 1043 (1986).
20. P. F. Lambert, B. A. Spalholz, P. M. Howley, *ibid.* **50**, 69 (1987); N. L. Hubbert, J. T. Schiller, D. R. Lowy, E. J. Androphy, *Proc. Natl. Acad. Sci. U.S.A.* **85**, 5864 (1988).
21. K. W. Y. Cho *et al.*, *EMBO J.* **7**, 2139 (1990); C. V. E. Wright, K. W. Y. Cho, J. Hardwicke, R. H. Collins, E. M. DeRobertis, *Cell* **59**, 81 (1990).
22. B. L. Weber, E. H. Westin, M. F. Clarke, *Science* **249**, 1291 (1990).
23. T. Mitsuhashi, G. E. Tennyson, V. M. Nikodem, *Proc. Natl. Acad. Sci. U.S.A.* **85**, 5804 (1988); S. Izumo and V. Mahdavi, *Nature* **334**, 539 (1988); R. J. Koenig *et al.*, *ibid* **337**, 659 (1989).
24. X.-H. Sun and D. Baltimore, *Cell* **64**, 459 (1991).
25. M. Mercola, J. Goverman, C. Mirell, K. Calame, *Science* **227**, 266 (1985).
26. Confluent plates of NIH 3T3 cells were passaged (1:10) 2 days before transfection by calcium phosphate coprecipitation as described (*25*). CAT activity was normalized for transfection efficiency by the cotransfection of an expression construct that contained the human growth hormone cDNA (Allegro, San Juan Capistrano, CA) in all transfections. Hormone secreted into the medium was quantitated by radioimmunoassay.
27. C. Roman, J. S. Platero, J. Shuman, K. Calame, *Genes Dev.* **4**, 1404 (1990).
28. L. Ramakrishnan and N. Rosenberg, *Mol. Cell. Biol.* **8**, 5216 (1988).

29. We thank T. Kadesch for supplying the pSV2A and CAT reporter constructs and for sharing confidential information before publication; M. Kiledjian for the plasmid pGEM3Lδ147cat; H. Singh for pBS-ATG; colleagues S. Goff, M. Gottesman, D. Shore, C. Cooper, and S. Artandi for critical reading of this manuscript; U. Beauchamp in the DNA sequencing facility; and S. Julien for technical assistance. Supported by USPHS grants RO1GM28361 and RO1CA38571; partially supported by a National Institute of General Medical Sciences Cellular and Molecular Biology Predoctoral Training Grant (C.R.).

21 May 1991; accepted 14 June 1991

A Mutation in the Amyloid Precursor Protein Associated with Hereditary Alzheimer's Disease

JILL MURRELL, MARTIN FARLOW, BERNARDINO GHETTI, MERRILL D. BENSON*

Alzheimer's disease is a form of localized amyloidosis characterized by cerebral cortical amyloid plaques, neurofibrillary tangles, and amyloid deposits within the walls of leptomeningeal vessels. Although most cases of Alzheimer's disease are sporadic, kindreds with autosomal-dominant inheritance of the syndrome suggest that a single mutation may be important in pathogenesis. Direct sequencing of DNA from a family with autopsy-proven Alzheimer's disease revealed a single amino acid substitution (Phe for Val) in the transmembrane domain of the amyloid precursor protein. This mutation correlates with the presence of Alzheimer's disease in all patients in this study, and may be the inherited factor causing both amyloid fibril formation and dementia.

HEREDITARY OR FAMILIAL ALZHEIMER'S disease is an autosomal-dominant form of localized amyloidosis. Patients with hereditary Alzheimer's disease typically develop three pathologic lesions: (i) senile plaques in the cerebral cortex characterized by a central amyloid core surrounded by dystrophic neurites; (ii) neurofibrillary tangles; and (iii) congophilic angiopathy of the leptomeningeal vessels. The amyloid deposits in the senile plaques and in the blood vessel walls contain a fibril subunit protein of 39 to 43 amino acid residues (*1*), which is a portion of the carboxyl terminus of the amyloid precursor protein (APP). Sequence analysis of cDNA clones of APP has shown that there are multiple forms of mRNA which are the result of alternate splicing of a transcript from a single gene (*2–5*). Although the sequence of the APP gene from some patients with either sporadic or familial Alzheimer's disease is normal (*6–8*), a missense mutation in the membrane-spanning domain of the APP gene has been identified in patients from several families with familial Alzheimer's disease (*9, 10*).

We used genomic DNA from three generations of a family with classic early-onset autosomal-dominant Alzheimer's disease to determine whether the disease in this family is associated with a point mutation in the APP gene. We amplified and sequenced exon 15 of the APP gene using the polymerase chain reaction (PCR) (Fig. 1) (*7, 9, 11*).

Affected members of this family show clinical onset of disease with short-term

Indiana University School of Medicine, Departments of Medicine, Medical and Molecular Genetics, Neurology, Pathology, and the Veterans Affairs Richard L. Roudebush Medical Center Indianapolis, IN 46202.

*To whom correspondence should be addressed.